ORAL/POSTER PRESENTATION: ICF100555OR

TRANSITION FROM DUCTILE TO CLEAVAGE FRACTURE - EFFECT OF SPECIMEN SIZE AND MISMATCH

E. Østby[1], Z. L. Zhang[2], and C. Thaulow[1]

[1]Department of Machine Design and Materials Technology, Norwegian University of Science and Technology, N-7491, Trondheim, Norway
[2]SINTEF Materials Technology, N-7465, Trondheim, Norway

ABSTRACT

The effect of specimen size and mismatch on the possible transition from ductile crack growth to cleavage is studied for two different specimen geomtries by means of 2D FE analysis. For homogeneous specimen the crack growth resistance is little influenced by specimen size. The stress level displays stronger size dependence resulting in increasing probability of cleavage fracture with increasing specimen size. For mismatch situations the crack growth resistance is only clearly reduced in cases where the crack grows along the interface between the two materials. When crack growth deviation occurs the detrimental effect of mismatch is reduced both with regard to crack growth resistance and susceptibility to cleavage fracture. The crack growth deviation for mismatch cases is mostly dependent on the specimen geometry, and specimens loaded in bending show stronger tendency for deviation than specimen loaded in tension.

KEYWORDS

Ductile crack growth, Cleavage fracture, Size effect, Mismatch, Numerical simulation

INTRODUCTION

In the ductile to brittle transition region cleavage fracture in steels may be preceded by ductile crack growth. Recent progress in modelling of ductile crack growth, using either damage mechanics (see e.g. [1-2]) or cohesive zone models (see e.g. [3-4]), has brought better understanding of both the ductile and cleavage behaviour of steels in this region. Of special interest for the cleavage fracture susceptibility has been the observation that the stress level increases with ductile crack growth, and this has been used as one way of explaining why transition from ductile to cleavage crack growth may happen (see. e.g. [5-6]). In this paper we focus on two aspects regarding ductile crack growth in finite specimens. The first is the effect of the specimen size. The second aspect addressed is the effect of mismatch for cracks initially located on the interface between two materials with different yield stress. This latter aspect is of great interest for prediction of the behaviour of weldments, where often the most critical location of cracks is close to the fusion line between the weld metal and the Heat Affected Zone (HAZ)/base material.

MATERIALS AND FE-DETAILS

The two different finite geometries studied by means of 2D plane strain FE-analysis are shown in Figure 1. One is a shallow cracked specimen (a/W=0.15) loaded in tension, while the other is a deep cracked specimen (a/W=0.5) loaded in bending. The two different geometries are chosen to evaluate the effect of different

constraint levels. The one half of the specimen where the crack growth will take place is referred to as Mat 1, and is modelled as Gurson material. The other half is referred to as Mat 2, and a von Mises constitutive relation is used here. Referring to Figure 1. the mismatch ratio, m, between Mat 1 and Mat 2 is defined as:

$$m = \frac{\sigma_{0,2}}{\sigma_{0,1}} \tag{1}$$

where $\sigma_{0,1}$ and $\sigma_{0,2}$ is the yield stress of Mat 1 and 2, respectively. In the case of no mismatch m=1. The relation between plastic strain and flow stress used for Mat 2 and the matrix in Mat1 is on the form:

$$\bar{\sigma} = \sigma_0 \left(1 + \frac{\varepsilon_p}{\varepsilon_0} \right)^n \tag{2}$$

where $\bar{\sigma}$ is the flow stress, σ_0 is the yield stress, ε_p is the equivalent plastic strain, $\varepsilon_0=\sigma_0/E$ is the strain at yield, and n is the hardening exponent. The yield stress of Mat 1 is kept fixed at 400 N/mm^2 (with $E/\sigma_0=500$), while the yield stress in Mat 2 is varied according to (1). A value n=0.1 for the hardening exponent is used in all analyses. The yield function of the Gurson model has the following form:

$$\phi(q, \bar{\sigma}, f, \sigma_m) = \frac{q^2}{\bar{\sigma}^2} + 2q_1 f \cosh\left(\frac{3q_2\sigma_m}{2\bar{\sigma}} \right) - 1 - (q_1 f)^2 = 0 \tag{3}$$

where f is the void volume fraction, which is the average measure of the void-matrix aggregate, σ_m is the mean macroscopic stress, q is the conventional von Mises stress, σ is the flow stress of the matrix material. Values of $q_1=1.5$ and $q_2=1.0$ have been used here. An initial void volume fraction of $f_0=0.002$ is assumed. Further, the increase in void volume fraction is assumed to be solely due to growth of existing voids, and no void nucleation is introduced in the analyses. Void coalescence is predicted by a hardening modified version of Thomason's limit load criterion discussed in [7]. Details of the near tip FE mesh are shown in Figure 2. An area with uniformly shaped elements extends 4.8 mm ahead of the crack tip and 0.7 mm to each side of the interface between the two materials. The element size in this area is 0.05x0.1 mm, with the shortest side parallel to the interface. The reason for choosing an aspect ratio of 2 is that this strongly reduces oscillations in the stress field, due to additional constraint at the interface in the mismatch cases, found when using elements with aspect ratio close to 1.

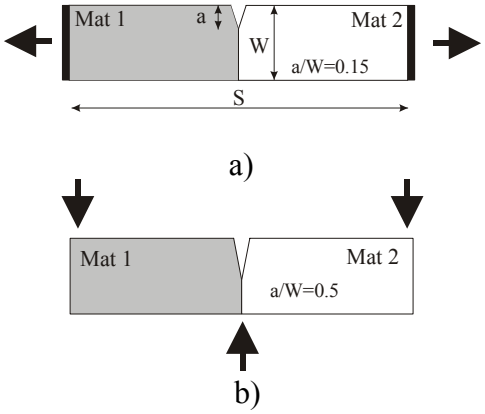

Figure 1. a) Shallow cracked (a/W=0.15) specimen loaded in tension. b) Deep cracked (a/W=0.5) specimen loaded in bending.

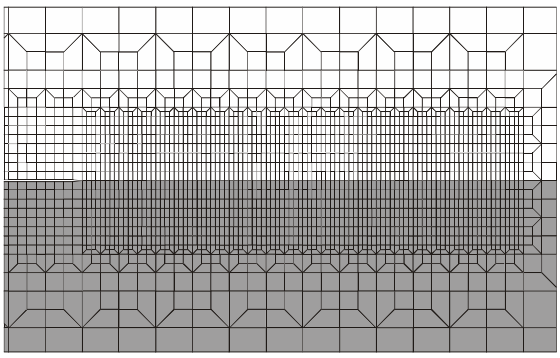

Figure 2. Near tip details of FE-mesh

SIZE EFFECT FOR HOMOGENOUS SPECIMENS

In this section we discuss the effect of specimen size in relation to ductile crack growth. Four different specimen thickness are used: W=25, 50, 100, and 200 mm. Figure 3 a) shows the J-Δa curves for different specimen thickness, W, from the numerical simulations of the shallow cracked specimen (a/W=0.15) loaded in tension. It is evident that the specimen size does not influence the crack growth resistance significantly. Figure 3 b) shows the J-Δa curves for the deep cracked bend specimens (a/W=0.5). Here it can be seen that initial part of the J-Δa curves, up to 1-1.5 mm of crack growth, is more or less independent of specimen size. After further crack growth a more pronounced effect of the specimen size can be seen, with less resistance to crack growth with increasing size. This observation is similar to what was reported in [8] for the same geometry.

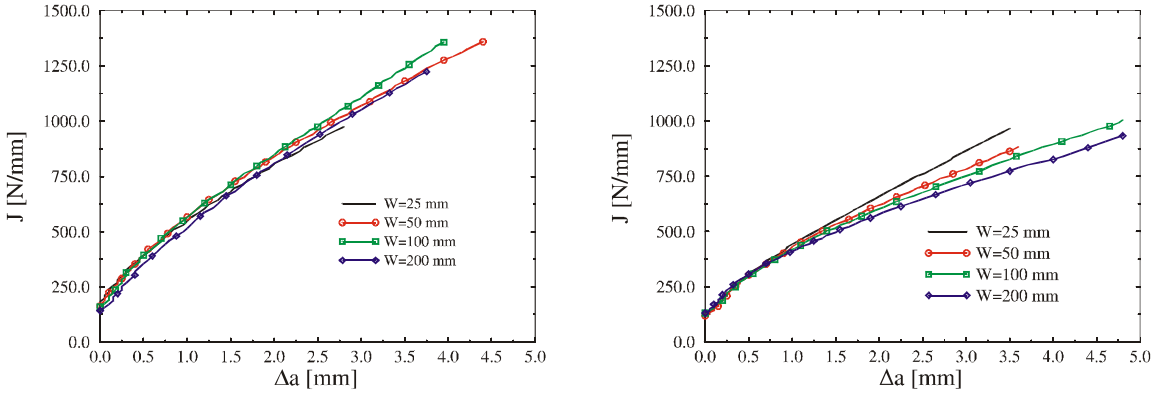

Figure 3. Effect of specimen size on the J-Δa curves. a) Shallow cracked specimen loaded in tension. b) Deep cracked specimen loaded in bending.

The normalised opening stress for different amounts of crack growth for the tensile specimen is compared for the different specimen sizes in Figure 4 a). For a fixed specimen size the peak stress is increasing with crack growth. For the largest specimen (W=200 mm) the increase is about 25% of the yield stress, and slightly less for the smaller specimen. It should also be observed that the major part of the increase in stress happens up to crack growth of about 1 mm, after which only a minor increase in peak stress is seen. An interesting point is the rather large size effect on the stress level, with about 100 N/mm^2 difference between the largest and smallest specimen. The evolution of the normalised opening stress for the deep cracked bend specimen is shown in Figure 4 b). For this high constraint geometry the relative increase in stress with crack growth is smaller than for the tensile specimen. There is also a tendency that the size dependence of the peak stress is somewhat reduced with crack growth. The area of highly stressed material will, however, increase more in the larger specimens due to smaller influence from the global bending field.

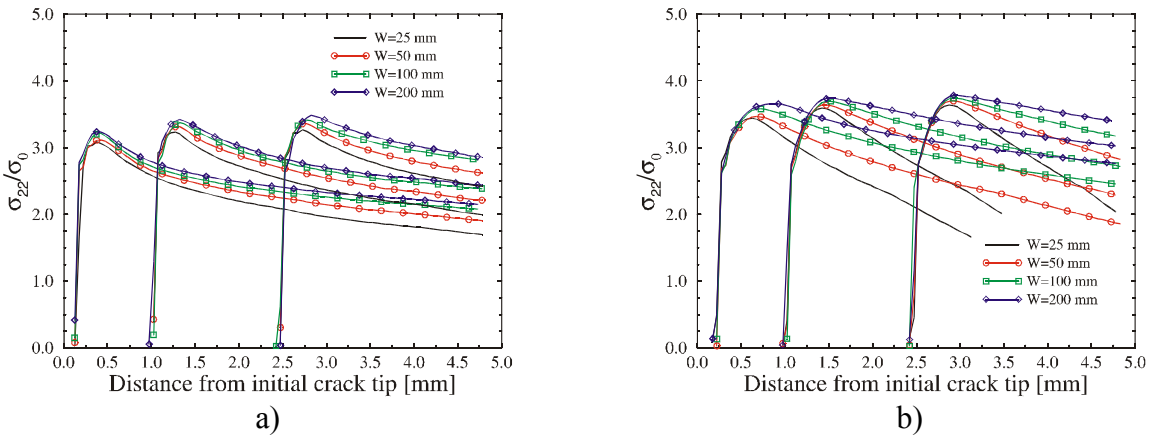

Figure 4. Evolution of normalised opening stress with crack growth. a) Shallow cracked specimen loaded in tension. b) Deep cracked specimen loaded in bending.

The size effect on the susceptibility to cleavage fracture is compared through the Weibull stress, σ_w, (Beremin [9]) calculated according to the following expression:

$$\sigma_w = \sqrt[m_w]{\frac{1}{v_0}\sum\left(\sigma_{1,i}\right)^{m_w} V_i} \tag{4}$$

where m_w is the Weibull modulus, v_0 is a scaling volume, $\sigma_{1,i}$ is the average principal stress in element i, and V_i is the volume of element i. The summation is performed over all elements actively yielding. Values of m_w=20 and v_0=0.001 mm^3 have been assumed. The evolution of the Weibull stress as a function of J for the tensile and bend specimens are shown in Figure 5 a) and b), respectively. From Figure 5 a) it can be seen that the Weibull stress is monotonically increasing with J. Also as expected from the stress fields the Weibull stress for a given J is increasing with increasing specimen size. The results thus indicate that the cleavage fracture probability will increase with increasing ductile crack growth, and that the brittle fracture probability for a given J is increasing with specimen size. Similar results are also seen for the bend specimen in Figure 5 b), however, with a stronger size effect due to the influence of the global bending field.

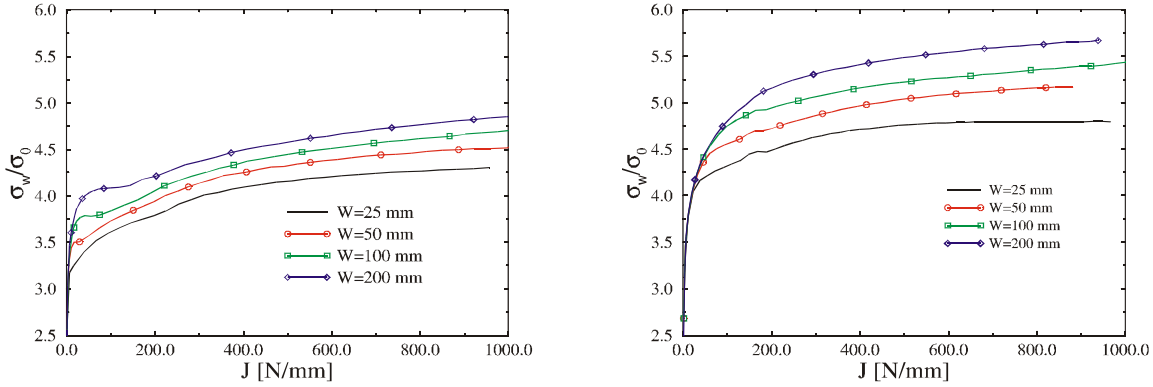

Figure 5. Effect of specimen size on evolution of normalised Weibull stress. a) Shallow cracked specimen loaded in tension. b) Deep cracked specimen loaded in bending

EFFECT OF YIELD STRESS MISMATCH

This section focuses on the effect of mismatch for cracks initially lying on the interface between two materials with different yield stress. The crack is assumed to grow in the material with the lowest yield stress. Three different levels of mismatch, m=1.125, 1,25, and 1.5, are considered both for the tensile and the bend specimen. The specimen thickness, W, is fixed at 50 mm. For the mismatch case the possibility of crack growth deviation away from the interface enters as a new feature compared to simulation of ductile crack growth in homogenous specimens. The effect of mismatch on the J-Δa curve and the crack growth path for the different mismatch levels are shown in Figure 6 a) and b), respectively, for the tensile specimen. From Figure 6 a) it can be seen that mismatch reduces the crack growth resistance. For the two lowest mismatch levels, m=1.125 and 1.25, the reduction compared to the homogenous specimen (m=1) is small. A reason for this can be seen from Figure 6 b) where it is observed that the crack growth does not follow the interface. For m=1.5, however, the reduction in crack growth resistance is significant, following from the fact that the crack grows along the interface. Figure 7 a) shows the effect of mismatch on the crack growth resistance for the bending case, and the crack growth paths are shown in Figure 7 b). By comparing Figure 6 b) and 7 b) it can be seen that the tendency for crack deviation due to mismatch is stronger for the bending than for the tensile specimen. The effect of this stronger tendency to crack deviation is seen on the resistance curves in Figure 7 a), where the curves for m=1.125 and 1.25 displays a slightly higher slope than for the

homogenous specimen. Initially the bend specimen with m=1.5 has crack growth along the interface (up to about 0.5 mm), after which a strong deviation of crack growth path is the case also for this mismatch level.

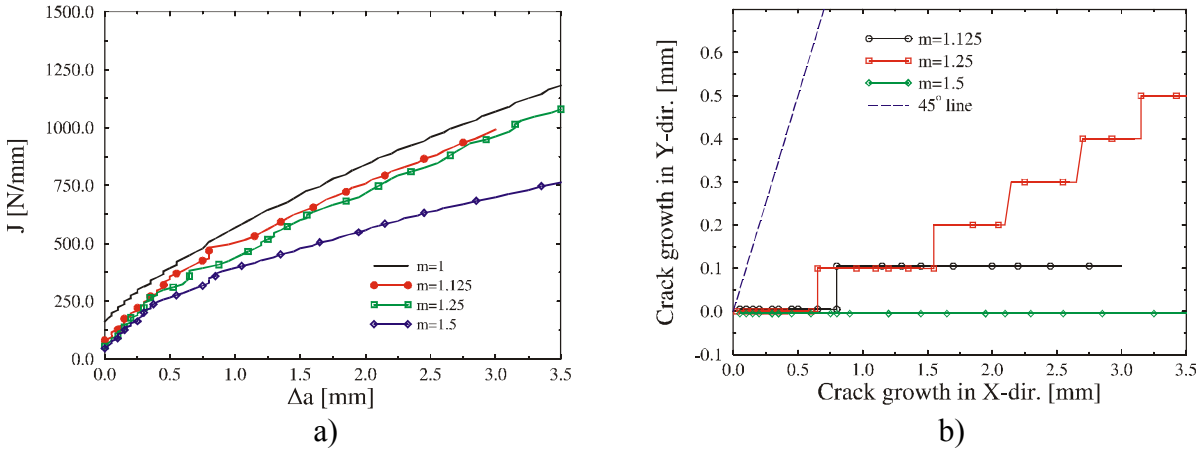

Figure 6. Effect of mismatch on ductile crack growth behaviour for shallow cracked specimen loaded in tension. a) J-Δa curves. b) Crack growth paths.

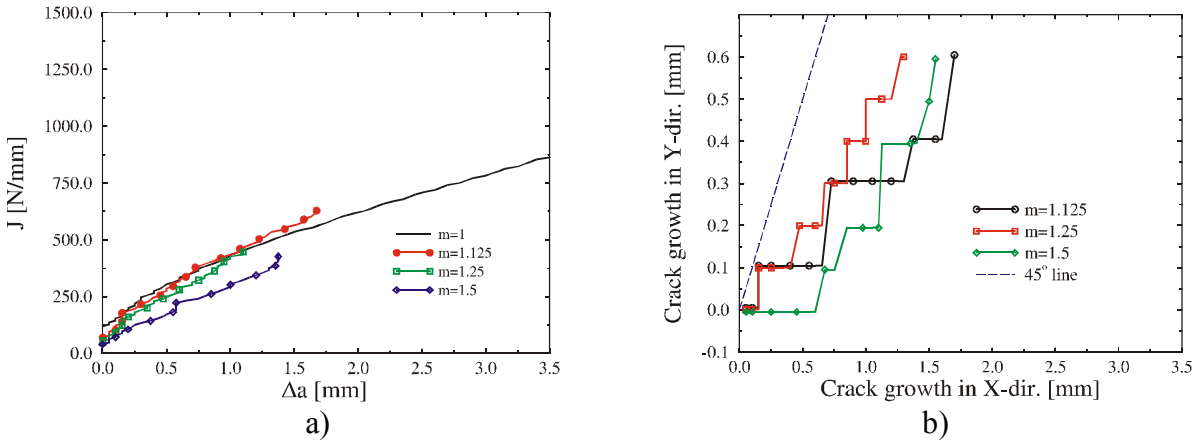

Figure 7. Effect of mismatch on ductile crack growth behaviour for deep cracked specimen loaded in bending. a) J-Δa curves. b) Crack growth paths.

The structure of the stress fields for growing cracks in mismatched specimens becomes complex due to the deviation of the crack growth away from the interface. The effect of mismatch on the brittle fracture susceptibility for ductile crack growth is only discussed through the Weibull stress here. Contribution to the Weibull stress for the mismatched specimens is only calculated in Mat 1, while for the case with m=1 the whole specimen is used. The results for the evolution of the Weibull stress for the different levels of mismatch are shown in Figure 8 a) for the tensile specimen and in Figure 8 b) for the bend specimen. For the tensile case a clear effect with increasing Weibull stress for increasing level of mismatch is seen. This indicates that a detrimental effect of mismatch should be expected on the susceptibility to cleavage fracture for ductile crack growth in specimens loaded in tension. The results for bending also indicate a detrimental effect of mismatch for low load levels. However, it can be seen that the Weibull stress for the mismatch cases displays a lower increase for increasing load compared to the homogenous specimen. Thus, when significant deviation of the crack growth occurs the detrimental effect of mismatch is reduced.

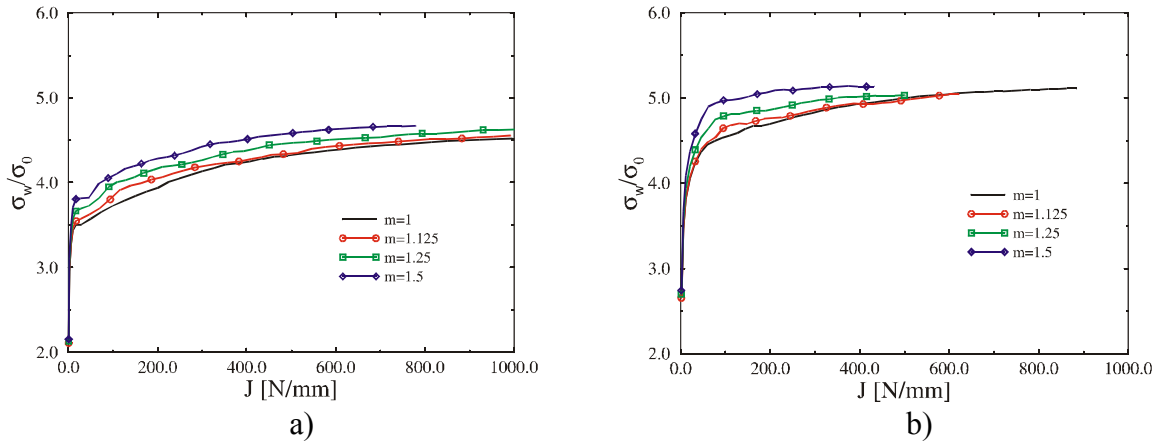

Figure 8. Effect of mismatch on the evolution of the Weibull stress. a) Shallow cracked specimens loaded in tension. b) Deep cracked specimens loaded in bending.

CONCLUDING REMARKS

The numerical simulations indicate that no unique stress field exists for ductile crack growth in a given specimen geometry, and the specimen size, together with the specimen geometry, will influence on the stress level. The size effect appears to be more important with regard to cleavage fracture susceptibility than for ductile crack growth resistance. As for stationary cracks, mismatch will also have a detrimental effect on cleavage fracture probability for interface cracks when ductile crack growth occurs. However, crack growth deviation away from the interface will reduce the detrimental effect of mismatch both for the cleavage fracture susceptibility and the resistance to ductile crack growth. This latter effect appears to be more pronounced for specimens loaded in bending compared to specimens loaded in tension.

ACKNOWLEDGEMENTS

The Norwegian Research Council and Statoil are gratefully acknowledged for their support of the research presented in this paper.

REFERENCES

1. Xia, L. and Shih, C. F., (1995) J. Mech. Phys. Solids, 43, 233
2. Xia, L. and Shih, C. F., (1995) J. Mech. Phys. Solids, 43, 1953
3. Tvergaard, V. and Hutchinson, J. W. (1992) J. Mech. Phys. 40, 1377
4. Tvergaard, V. and Hutchinson, J. W. (1994) Int. J. Solids Structures, 31, 823
5. Xia, L. and Shih, C. F., (1996) J. Mech. Phys. Solids, 44, 603
6. Ruggieri, C. and Dodds, R. H., (1996) Int. J. Fracture (1996), 79, 309
7. Zhang, Z. L., Thaulow, C. and Ødegård, J. (2000) Eng. Frac. Mech. 67, 155
8. Xia, L., Shih, F. C. Hutchinson, J. W., (1995) J. Mech. Phys. Solids, 43, 389
9. Beremin, F. M, (1983) Met. Trans. A, 14A, 2277